Reciprocal-space mapping of lateral single-crystal domains with grazing-incidence x-ray diffraction for tetracene on H/Si(001)

A. Tersigni,[1] X. R. Qin,[1,*] C.-Y. Kim,[2] R. A. Gordon,[3] and D. T. Jiang[1,†]

[1]*Department of Physics, Guelph-Waterloo Physics Institute, University of Guelph, Guelph, Ontario N1G 2W1, Canada*

[2]*Canadian Light Source, Saskatoon, Saskatchewan S7N 0X4, Canada*

[3]*Advanced Photon Source, Argonne National Laboratory, Argonne, Illinois 60439, USA*

(Received 31 August 2010; revised manuscript received 1 May 2011; published 15 July 2011)

We have measured in-plane single-crystal domain changes in size and shape for a tetracene film on H/Si(001)-2×1 as a function of film thickness and substrate step density using grazing-incidence x-ray diffraction (GIXD). The x-ray results reveal that the film is commensurate with the substrate along the **a** axis of the tetracene lattice (i.e., the longer base vector of the a-b plane unit cell). The preferred crystalline domain growth direction is found to be along the **b** axis (the shorter base vector of the unit cell). The single-crystal domain size is layer dependent and orders of magnitude smaller than a typical surface island observed using atomic-force microscopy (AFM). The domain size and shape are sensitive to the substrate step density and step anisotropy. The mechanism of substrate step influence on the domain properties has been discussed.

DOI: 10.1103/PhysRevB.84.035303 PACS number(s): 68.55.−a, 81.05.Fb, 61.05.C−, 68.37.Ps

I. INTRODUCTION

Since the demonstration of organic field-effect transistors (FETs), where a thin film of conjugated molecules acts as the semiconductor layer, the mechanism of charge transport has become a challenging issue for research.[1–6] Because the structure of molecular films and the transport properties are intimately related, fast-paced progress has been made on studying organic thin film growth and characterizing the structure and morphology of the thin films with multiple techniques.[3,7–11] It has been shown that in organic FETs, the charge transport is thickness dependent and only several or even a few molecular layers next to the molecule-substrate interface dominate the charge transport.[12,13] Despite the efforts in forming the high-quality films and in correlating the morphology and structure of an organic film to the carrier mobility,[7–14] few experimental studies have addressed the structure properties of single-crystal domains, the fundamental crystallites within the film, which should be crucial in bridging the structure and transport properties of organic films. This requires the ability to detect the in-plane domain size and orientation in an organic film, especially the layer-dependent domain structure of the initial film, which, to our knowledge, has not been previously demonstrated.

In the present study, we have employed grazing-incidence x-ray diffraction (GIXD) for reciprocal-space mapping of the in-plane single-crystal domains of organic films, using a tetracene film on H-Si(001)-2×1 surface as a prototypical system. Tetracene ($C_{18}H_{12}$) consists of four fused benzene rings (Fig. 1), and is a promising candidate in organic FETs and light-emitting transistors.[4,15] The hydrogen-terminated Si(001)-2×1 surface provides a structurally well-defined and inert substrate template,[16] which is a well-suited surface for fundamental research. In our previous work, we have shown that a layered tetracene film[17] on H/Si(001) is commensurate with the substrate along one dimension,[18] and that the molecules within the film layers take on a herringbone formation that is similar to the bulk structure. In this study, we report the registration of the film lattice to that of the silicon substrate and the dependence of the domain size on the layer thickness, and also that the in-plane domain size and shape are sensitive to the substrate step density and step anisotropy. We demonstrate that GIXD with synchrotron radiation can be used to characterize ultrathin organic crystalline films; its sensitivity to the microscopic changes of the substrate allows us to gain insight into the initial film structure formation mechanisms.

II. EXPERIMENTAL

Sample preparation was carried out in a two-chamber ultrahigh vacuum (UHV) system. The hydrogen-terminated Si(001) was prepared as in our earlier report,[18] by thermal-cleaning the silicon wafer at ∼1470 K for ∼1 min in the first chamber (base pressure of $\sim 1\times 10^{-10}$ torr), and then using a hot tungsten filament (∼1800 K) to generate atomic hydrogen while back-filling the chamber with molecular hydrogen ($\sim 10^{-6}$ torr) for 20 min to form a silicon monohydride 2×1 surface at ∼600 K. Two types of silicon substrates were used, with miscut angles of 0.03° and 0.3° toward the [110] direction (i.e., the surface normal deviates from the lattice [001] and inclines towards the [110] direction by these angular amounts) and hence terrace widths of ∼2600 and 260 Å, respectively.

Monolayers (ML) of tetracene films were grown in the second chamber (base pressure of $\sim 3\times 10^{-9}$ torr) by thermal evaporation of tetracene from an alumina crucible heated by a tungsten basket, at a deposition rate of 0.8 ML/min. A quartz crystal microbalance (QCM) was used to monitor the deposition rate which was controlled by adjusting the temperature of the crucible. The QCM reading has previously been calibrated by atomic-force microscopy (AFM) imaging. The tetracene films described here are 1.5, 4, and 12 ML in thickness.

GIXD measurements were performed *ex situ* in He environment at beamline 20ID-C, Advanced Photon Source (APS) at Argonne National Laboratory, and at HXMA beamline, the Canadian Light Source (CLS). In both cases multicircle Huber diffractometers were used. The x-ray photon energies used were 10 keV and 20 keV at APS and CLS, respectively. For the experiment geometry of the results reported here, the

 ©2011 American Physical Society

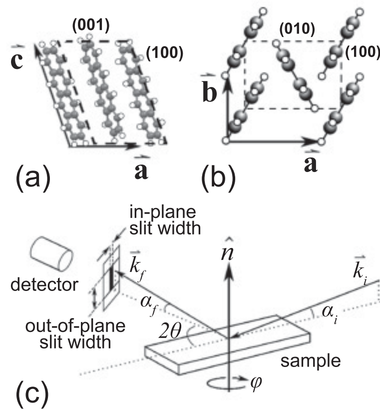

FIG. 1. Tetracene crystalline structure: (a) side view; (b) top view. Carbon atoms are shown in black, hydrogen in white. (c) Scheme illustrating the experimental set up of GIXD.

diffraction plane is vertical to the synchrotron storage ring plane. In the GIXD experiments, depicted in Fig. 1(c), the incident beam angle α_i was set to approximately two-thirds of the critical angle for total reflection. A set of collimating slits [not shown in Fig. 1(c)] placed upstream from the sample was used to define the incident beam profile, and to ensure acceptable collimation. For example, for the measurements performed at the APS 20ID-C, the incident beam collimation was $\sim$6 μ rad in plane with respect to the sample surface. The diffracted beam was measured with a point detector placed behind a second set of slits, with an in-plane slit width of 1 mrad, and an out-of-plane slit width of 10 mrad to integrate along the q_z (the z component of the x-ray scattering vector **q** in reciprocal space) direction in order to maximize the intensity detection. With this setup, the in-plane resolution in reciprocal space is primarily limited by the detector slits and finite sample illumination area under the grazing-incidence geometry. By measuring the intensity profile of silicon surface (111) diffraction peaks, the radial and transverse resolution in the q_{xy} plane are estimated to be 5×10^{-3} Å^{-1} and 10^{-4} Å^{-1}, respectively. Since peak width measurements in this study depend on sample and peak orientation, the actual resolutions for these measurements tend to be better than this. Therefore, the radial resolution represents the worst-case scenario. For the reciprocal-space maps shown in this work the x-ray beam linear polarization is along the surface normal. All the quantitative analysis in this work is based on the data acquired under these conditions. For the x-ray diffraction results presented here, in order to prevent radiation damage to the sample during exposure to the x-ray beam, samples were held in a chamber which was constantly being flushed with helium gas at atmospheric pressure. No measurable systematic decay of the intensities of the diffraction peaks was detected in these experiments, even after several hours of exposure to the x-ray beam.

Since all the domains are orientated with the [001] direction normal to the substrate surface (i.e., standing molecules),[18,19] for our GIXD experiment, only diffraction peaks corresponding to the tetracene a-b plane were sought. To estimate domain sizes, two-dimensional (2D) reciprocal-space mapping of the peak intensity profiles was performed by rasterizing the diffracted beam intensity measurements over a grid of 2θ and φ values. The resulting grid of measurements was then converted into reciprocal-space coordinates to produce a 2D cross section of the peak in the lateral reciprocal space parallel to the substrate surface.

III. RESULTS AND DISCUSSIONS

Our GIXD data show that there are dominantly two sets of discrete in-plane Bragg peaks existent for the films, suggesting that two orthogonal but otherwise identical lattice orientations or domains are dominant in the coalesced tetracene monolayers. From fitting these Bragg reflection positions, the in-plane film lattice is found to have $|\mathbf{a}| = 7.70 \pm 0.02$ Å, $|\mathbf{b}| = 5.93 \pm 0.02$ Å, and $\gamma = 90.0^\circ \pm 0.2^\circ$. The result on $|\mathbf{a}|$ is in agreement with the previous assessment based on the STM results [18] which indicate the film lattice is commensurate with the substrate lattice along the **a** direction [Fig. 1(b)]. However, the x-ray result for $|\mathbf{b}|$ suggests the film lattice is incommensurate with the substrate along the **b** direction.

Figure 2(a) presents a reciprocal-space map of GIXD peaks detected for a 4-ML tetracene film grown on a 0.03°-miscut substrate. Black dots represent the locations where the in-plane diffraction peaks are found, and some 2D-contour plots of selected peaks are overlaid on their respective coordinates. Based on intensity calculations for the bulk structure of tetracene[20] our detected peaks are consistent with the approximate expected positions of the bulk ($\bar{1}10$), ($\bar{2}10$), and (200) peaks. These peaks are expected to have the most significant diffraction intensity (based on the unit-cell structure factor) within the range of angles examined. Evidently, there are two types of unit-cell orientations perpendicular to each other, as illustrated by red and green dashed lines. All of the detected peaks of significant intensity match one of these two orientations. These orientations are such that the **b** direction of the tetracene film is aligned either parallel or perpendicular to the [110] direction of the substrate lattice.

Note that while the structure factor calculations predict that the (110) and the (210) peaks should be insignificant in intensity as compared with the ($\bar{1}10$) and ($\bar{2}10$) peaks, respectively, we still detected peaks with significant intensity at these positions. For instance, in surveying line scans (at a fixed scattering angle scanning through sample surface azimuth angle), it was found that the nominal (11) in-plane peak in Fig. 2(a) (the unmapped black spot at the end of the red $\mathbf{b}^*$ vector) has a similar peak intensity as that of the mapped ($\bar{1}1$)peak, with a difference $<1\%$. On the other hand, according to the estimated structure factor using the bulk tetracene lattice parameters, the expected (11) peak intensity should be only $\sim$8% of that of the ($\bar{1}1$) peak. This indicates that there exists a significant number of domains in the film with their $\mathbf{a}^*$ axis direction inverted 180° from the $\mathbf{a}^*$ direction shown in Fig. 2(a). Similar observations hold true for the mapped peak at the nominal (21) position [indexed as the ($\bar{2}1$) peak for the red domains in Fig. 2(a)], which would be insignificant (two orders of magnitude weaker) according to the structure factor estimation. Therefore, for each of the two apparent domain orientations that we detect, there could be three others associated with it, each representing a domain after rotation of 180° about the **a**, **b**, or **c** axes, and they

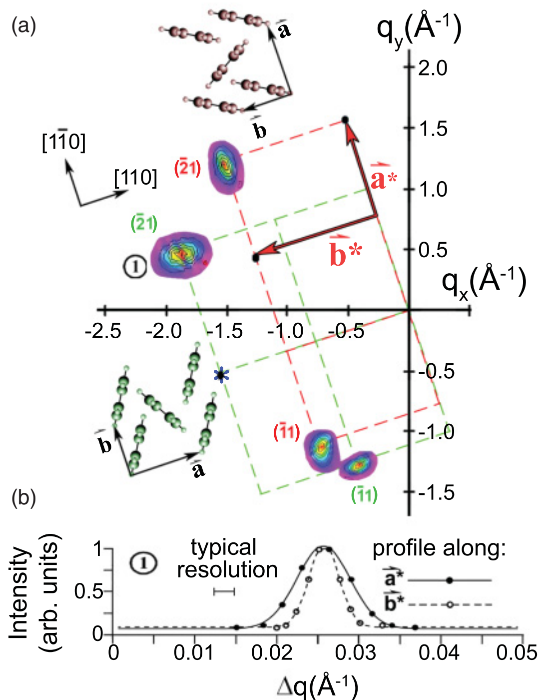

FIG. 2. (Color) (a) 2D reciprocal-space map of measured GIXD peaks for a 4-ML tetracene film on a 0.03°-miscut H/Si(001) substrate. The red and green dashed lines indicate the two types of unit cells with the corresponding molecular lattices shown, and the projections of reciprocal lattice vectors $\mathbf{a}^*$ and $\mathbf{b}^*$ onto the q_x-q_y plane are indicated. The indices of the peaks indicate the most significant in-plane diffractions, given the coexistence of domains with either $\mathbf{a}^*$ or $\mathbf{b}^*$ rotated 180° (see text for more discussion). Substrate lattice coordinates are indicated on the left side, and the projected position of the bulk silicon (111) peak is indicated with a blue star. The positions of all detected GIXD peaks of significant intensity are indicated by black dots. Contour plots of selected peaks are enlarged in a scale of 30 : 1 and overlaid on the respective coordinates. (b) Line profiles showing cross sections of the numbered peak; each curve is a least-squares fit to the raw data. Δq indicates a relative position in the reciprocal space. The typical resolution shown is the average of the radial and transverse resolutions.

would have the same in-plane lattice constants, and would thus be indistinguishable in the in-plane diffraction data. In other words, for the red and green domains shown in Fig. 2(a), there exist equivalent domains with $\mathbf{a}^*$ or $\mathbf{b}^*$ pointing in opposite directions, respectively. In indexing of the in-plane diffraction peaks, we marked only the indices which are the most significant in intensity according to the estimation based on calculated structure factors, e.g., the marked ($\bar{2}$1) peak in Fig. 2(a) is in fact at the position of peak (21) for the particular $\mathbf{a}^*$ and $\mathbf{b}^*$ orientations shown in the figure.

The fact that the two domains follow the orientations of the substrate lattice is in good agreement with our real-space studies[18] that the tetracene film is commensurate with the silicon substrate along the film **a** axis, suggesting a nonnegligible influence of the substrate lattice in the film nucleation and growth. The obtained two-domain GIXD pattern [Fig. 2(a)] is in clear contrast to the case of randomly oriented crystalline domains (i.e., 2D powder) from which a ring-type diffraction pattern would be produced. It is this highly crystallized organic film that permits the characterization of the lateral properties of single-crystal domains.

Figure 2(b) displays cross sections of a peak intensity profile, which exhibits apparent anisotropy in size for the crystalline domain. The peak has the narrowest width along the $\mathbf{b}^*$ axis, so that the longest domain length is along the **b** direction, the direction normal to the bulk (010) surface. Such domain-size anisotropy has been found for all three film thicknesses and on all substrates used in this work, indicating an intrinsic tendency of forming the crystalline structure most favorably along the **b** direction. Theoretical studies on pentacene crystals show that the molecular binding energies (E_b) at the in-plane facets have the following relation: E_b (010) > E_b (100) > E_b (other facets). The corresponding growth velocity of the (010) step is thus higher than the (100) step (i.e., the growth probability along the **b** axis is higher than that along the **a** axis), leading to a longer domain length along the **b** axis.[19] Because of the structural similarity between pentacene and tetracene crystals, the obtained domain-size anisotropy suggests similar energetics for the tetracene crystallites and indicates that molecular self-assembling plays an important role in the single-crystal domain growth.

To quantitatively evaluate the average domain sizes under different film thickness and substrate conditions, we further analyze the 2D-contour plots by removing the instrumentation broadening (a point-spread function) in the radial direction through deconvolution of the raw data and extracting the intrinsic peak profiles.[21] The deconvolution step is used to estimate the variance in the domain-size values from different data analysis processes. The main conclusions presented here can also be drawn from the raw data without the deconvolution step. The extent to which deconvolution changes the quantitative results is reflected in our error estimates. Both film-domain shape and size are linked to the diffraction peak profile via Fourier transform, and hence the shape and size of the detected diffraction peaks will be affected by the distribution of actual shapes and sizes of the tetracene domains within the film. Using the Scherrer equation,[22] we provide estimates for the average domain size along a particular crystal axis as $2\pi/\Delta Q$, where ΔQ is the width of the diffraction peak along that axis. Our estimations for the average domain sizes along the **a** and **b** directions are listed in Table I.

We find that on a 0.03°-miscut substrate, the average domain sizes (L_b and L_a in Table I) tend to increase with the film thickness from 1.5 to 4 ML, but apparently decrease for thicker films (e.g., 12 ML). These results show directly that the domain sizes are layer dependent, and illustrate two points: (1) The second-layer domains are larger than the first-layer domains, so that the average domain sizes increase with the film thickness in early growth; (2) the fact that the domain sizes decrease for the thicker films strongly suggests a clear change in the nucleation density (or growth mode) as the growth proceeds. Such domain-size changes are consistent with our earlier work, in which we showed that the initial film (<2 ML) involves certain disorder in the molecular packing, and that a significant amount of highly crystallized structure emerges at nominal coverage of 3 ML.[18] Presumably, the initial packing disorder could be attributed to the higher density of domain boundaries (i.e., smaller domain sizes) in the first layer than

TABLE I. Estimates of the average single-crystal domain size within the tetracene films, based on the widths of the diffraction peaks in reciprocal space. The estimation error is mainly based on the reading error and the error in estimating the point-spread function. Typical ranges of uncertainties are ±20% for 1.5 ML, ±15% for 4 ML, and ±10% for 12 ML films, respectively.

		b // steps			**b** ⊥ steps		
		Domain size		Ratio	Domain size		Ratio
Substrate	Thickness	L_a (Å)	L_b (Å)	(L_b/L_a)	L_a (Å)	L_b (Å)	(L_b/L_a)
0.03° miscut (terrace: 2600 Å)	1.5 ML	1020	1400	1.37	1030	1300	1.26
	4 ML	1130	2200	1.95	900	1460	1.62
	12 ML	410	920	2.24	420	880	2.10
0.3° miscut (terrace: 260 Å)	1.5 ML	560	950	1.70	640	760	1.19
	4 ML	530	1040	1.96	550	640	1.16

in the second layer, and we believe that the maximum domain sizes are likely formed around 3–4ML.

Comparison of the domain sizes (L_b and L_a) and the surface topography images (Fig. 3) reveals that tetracene monolayer islands are not single crystals, but composed of numerous crystallites of the two types of single-crystal domains. Figures 3(a) and 3(b) show AFM images of 4-ML tetracene films grown on both 0.03°- and 0.3°-miscut substrates, respectively. The top surface island sizes appear to be 10–40 μm which is approximately two orders of magnitude larger than the average domain sizes estimated from the widths of the in-plane diffraction peaks. Such an extremely large difference in size between islands and domains is a result of kinetic growth processes in conjunction with limited molecule self-assembling. As shown in previous works,[7,17,23] the initial organic film growth is facilitated by a diffusion-limited-aggregation (DLA)[24] (hit-and-stick) type mechanism, and by growth-front smoothing (island edge diffusion) mechanism at elevated temperatures. The existence of the single-crystal domains should be related to the latter (thermodynamic) mechanism, while the area density (or the size) of the domains is related to the former, which is sensitive to the kinetic growth conditions. The high deposition rate we used in order to achieve a layered film morphology[17] would thus be the primary limiting factor for the domain sizes.

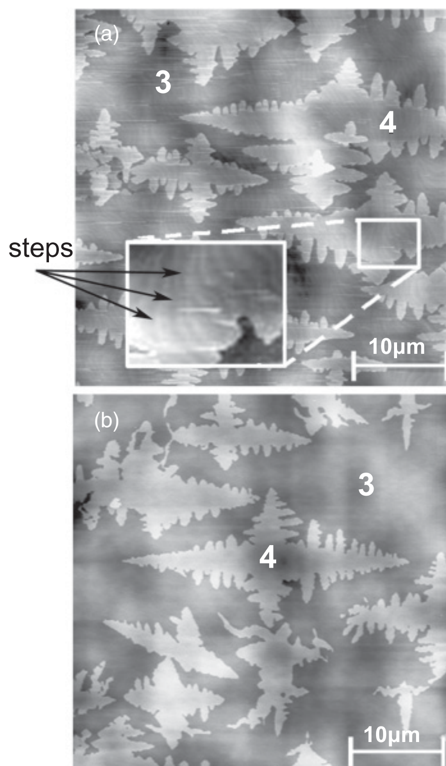

FIG. 3. AFM image of a 4-ML film on H-Si(001) with the substrate miscut angle of (a) 0.03° and (b) 0.3°. The third and fourth layers are marked by 3 and 4, respectively.

Because the formation of crystalline domains is driven by thermodynamics while the formation of topographical islands may not be dominated by energetic reasons, the preferred growth directions for these two structures could be different. Recent work[23,25] with pentacene on silicon substrates shows that the islands are always elongated along the **a** direction [i.e., the longer base vector of the a-b plane unit cell, see Fig. 1(b) for definition], which has been interpreted as due to kinetic preference in growth. While this kinetic result could also be true for tetracene island growth, considering the structural similarity between pentacene and tetracene crystals, our results on the domain-shape anisotropy clearly indicate that the crystalline lattice preferably grows along the **b** direction [i.e., the shorter base vector of the a-b plane unit cell, see Fig. 1(b) for definition].

Notice that for the same coverage (4-ML) films, the single-crystal domain sizes decrease sensitively with the increasing miscut angle (i.e., the increasing substrate step density). As listed in Table I, decreasing the terrace width from ∼2600 to ∼260 Å has the effect of reducing the average domain size by nearly a factor of 2. However, in contrast, the top surface islands from AFM imaging (Fig. 3) appear similar in size and shape for both substrates, insensitive to the change in the substrate step density.

To understand the apparent discrepancy between the x-ray and AFM results, we suggest that substrate steps may help to induce domain boundaries in the tetracene film. Because a Si(001) surface step is roughly 10% of the height of a single layer of upright tetracene molecules, the molecules from both sides of a substrate step are vertically shifted with respect to one another, which would weaken the interaction between these molecules due to the contact area being reduced. This vertical shift is evident in AFM topographs of the top film surface, through which the substrate steps are clearly visible (see inset in Fig. 3). The visible-step image suggests that

the tetracene film tends to conform to the substrate, even across substrate atomic steps. Hence a certain amount of disruption in the crystal structure may occur at substrate steps forming domain boundaries, resulting in effectively smaller single-crystal domains indicated by the x-ray results. Note that on the high-step-density substrate, our domain size estimates tend to be larger than the average terrace width, indicating that, despite the vertical shifting in the film lattice that is induced by the substrate steps, there is still some degree of correlation in the in-plane lattice registration across the substrate steps.

We further find that the choice of step orientation can induce domain growth anisotropy. Note that in our samples, the miscut is towards the silicon [110] direction. Therefore the substrate steps separate adjacent silicon terraces which alternate between having silicon dimer rows oriented parallel and perpendicular to the steps. Figure 4(a) displays a reciprocal-space map of the diffraction peaks for a 4-ML film grown on a 0.3°-miscut substrate. From Fig. 4(a), as compared with Fig. 2(a), the step influence on domain shape is clearly seen in the shapes of the diffraction peaks. First, for domains oriented with the preferred growth direction (i.e., the **b** axis) perpendicular to the substrate steps, the diffraction peaks [e.g., the peak labeled "1" in Fig. 4(a)] appear significantly more isotropic than the case shown in Fig. 2(a) (i.e., the aspect ratio of L_b/L_a=1.16 for high miscut vs 1.62 for low miscut; see Table I), suggesting that the preference for growth in the **b** direction has been diminished by the presence of the substrate steps. Second, for domains oriented with the **b** axis parallel to the substrate steps, the diffraction peaks [e.g., the peak labeled "2" in Fig. 4(a)] show virtually no change in the aspect ratio (1.96) compared with the case shown in Fig. 2(a) (1.95), indicating that the preferred growth direction has been preserved for these domains. Lastly, the aspect ratio difference for the two types of domains dramatically increases with the miscut angle, from 0.33 (=1.95–1.62) for a 0.03°-miscut substrate to 0.80 (=1.96–1.16) for a 0.3°-miscut substrate. In other words, significant step anisotropy in the substrate substantially enhances the shape difference between the two types of domains, depending on the preferred domain growth direction relative to the substrate step orientation.

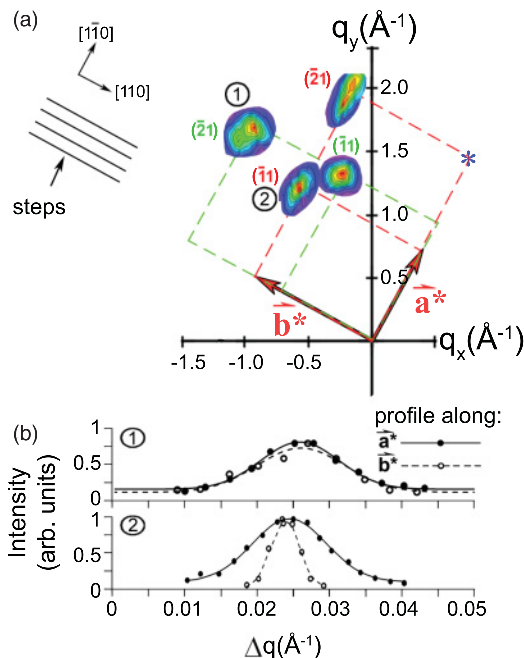

FIG. 4. (Color) (a) 2D reciprocal-space map of measured GIXD peaks for a 4-ML tetracene film on a 0.3°-miscut substrate; the contour plots are enlarged in a scale of 15:1. Substrate steps and lattice orientations are indicated at the upper left corner, and the projected position of the bulk silicon (111) peak is indicated with a blue star. (b) Cross sections of the numbered peaks (labeled by 1 and 2). Notations and resolutions are as in Fig. 2.

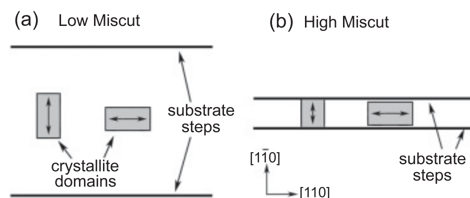

FIG. 5. Schematic illustrations of a possible step-density influence on the domain formation. A double arrow for each crystallite indicates the b axis. Note that in our samples, the miscut is towards the silicon [110] direction.

These observations are consistent with our hypothesis that the substrate steps may help to induce domain boundaries. As illustrated in Fig. 5, when the step spacing (or the terrace width) is much larger than the average domain sizes (i.e., low-miscut case), the aspect ratios for the two types of domains tends to be similar, indicating that molecular self-assembling in the domain formation is not significantly influenced by the steps here. When the step spacing is comparable to the domain size (i.e., high-miscut case), domains oriented with the **b** axis (indicated with arrows) parallel to the steps are not prevented from growing along their preferred growth direction; however, domains oriented with the **b** axis perpendicular to the substrate steps would have a certain probability to be confined in the preferred growth direction, as shown by a more isotropic domain shape, indicating that the substrate roughness inevitably plays a role in the domain growth. The domain-shape anisotropy shown is closely related to the choice of miscut direction (i.e., the choice of step orientation), even though the two dominant orientations of the film lattice are fixed with respect to the substrate lattice (due to the one-dimensional registry to the substrate). Presumably, one may control the domain shapes by the step orientation to some degree.

Besides the difference in the domain-shape anisotropy discussed here, the higher degree miscut angle at 0.3° (or higher substrate step density) also leads to generally smaller domain dimensions when compared with the counterparts in the 0.03°-miscut case (Table I). This may be related to the meandering of the steps, induced by imperfect miscut orientation of the substrates or annealing effects in stripping the native oxides of the substrate. Microscopically the step meandering would lead to a step edge alternatively along the [110] and [1$\bar{1}$0] directions, and the latter part could induce a limiting effect on domain size, as explained by the model in Fig. 5.

IV. CONCLUSIONS

We have measured in-plane single-crystal domain changes in size and shape for a tetracene film on H/Si(001)-2×1 as a function of film thickness and substrate step density using grazing-incidence x-ray diffraction. GIXD results reveal that the film is commensurate with the substrate along the **a** direction of the tetracene lattice (i.e., the longer base vector of the a-b plane unit cell). With GIXD and AFM, we demonstrate that a single-crystal domain in these films can be orders of magnitude smaller than a surface island. Two-dimensional reciprocal-space mapping of the diffraction peaks shows an anisotropy in the domain shape with a preferred growth along the **b** direction (i.e., the shorter base vector of the *a-b* plane unit cell), consistent with the energetics of molecular self-assembling. For low-miscut substrates, the domain sizes increase with the coverage initially, and decrease after a certain thickness. The domain sizes and anisotropy can be influenced by the substrate steps, which has been interpreted such that the steps have certain probability to introduce domain boundaries at the first layer and may affect the homoepitaxial layers grown above, influencing several monolayers adjacent to the substrate, which is highly relevant to the nature of the accumulation layer in organic FETs.

ACKNOWLEDGMENTS

The authors are grateful for useful discussions with Jim Britten. Q. Xiao, T. Regier, and N. Chen are acknowledged for assistance in data acquisition. This work was supported by NSERC of Canada through Discovery Grants to X.R.Q. and D.T.J. Use of the HXMA beamline at the CLS is supported by NSERC, NRC, CIHR, and the University of Saskatchewan. Use of the PNC/XOR facilities at the APS was supported by the U.S. Department of Energy, Office of Science, Office of Basic Energy Sciences, under Contract No. DE-AC02-06CH11357 and by a major facilities access grant from NSERC.

[*]xqin@uoguelph.ca
[†]djiang@uoguelph.ca
[1] S. R. Forrest, Nature **428**, 911 (2004).
[2] F. Schreiber, Phys. Status Solidi **201**, 1037 (2004).
[3] G. Witte and Ch. Wöll, J. Mater. Res. **19**, 1889 (2004).
[4] M. Muccini, Nat. Mater. **5**, 605 (2006).
[5] C. D. Dimitrakapoulos and P. R. L. Malenfant, Adv. Mater. **14**, 99 (2002).
[6] D. J. Gundlach, Y.-Y. Lin, T. N. Jackson, S. F. Nelson, and D. G. Schlom, IEEE Electron Device Lett. **18**, 87 (1997).
[7] F.-J. Meyer zu Heringdorf, M. C. Reuter, and R. M. Tromp, Nature (London) **412**, 517 (2001).
[8] R. Ruiz, D. Choudhary, B. Nickel, T. Toccoli, K. C. Chang, A. C. Mayer, P. Clancy, J. M. Blakely, R. L. Headrick, S. Iannotta, and G. G. Malliaras, Chem. Mater. **16**, 4497 (2004); R. Ruiz, A. C. Mayer, G. G. Malliaras, B. Nickel, G. Scoles, A. Kazimirov, H. Kim, R. L. Headrick, and Z. Islam, Appl. Phys. Lett. **21**, 4926 (2004).
[9] S. E. Fritz, S. M. Martin, C. D. Frisbie, M. D. Ward, and M. F. Toney, J. Am. Chem. Soc. **126**, 4084 (2004).
[10] H. Yang, T. J. Shin, M. M. Ling, K. Cho, C. Y. Ryu, and Z. Bao, J. Am. Chem. Soc. **127**, 11542 (2005).
[11] G. Horowitz and M. Hajlaoui, Adv. Mater. **12**, 1046 (2000).
[12] F. Dinelli, M. Murgia, P. Levy, M. Cavallini, and F. Biscarini, Phys. Rev. Lett. **92**, 116802 (2004).
[13] R. Ruiz, A. Papadimitratos, A. C. Mayer, and G. Malliaras, Adv. Mater. **17**, 1795 (2005).
[14] F. Cicoira, C. Santato, F. Dinelli, M. Murgia, M. A. Loi, F. Biscarini, R. Zamboni, P. Heremans, and M. Muccini, Adv. Funct. Mater. **15**, 375 (2005).
[15] A. Hepp, H. Heil, W. Weise, M. Ahles, R. Schmechel, and H. von Seggern, Phys. Rev. Lett. **91**, 157406 (2003).
[16] J. J. Boland, Phys. Rev. Lett. **65**, 3325 (1990); **67**, 1539 (1991).
[17] J. Shi and X. R. Qin, Phys. Rev. B **73**, 121303(R)(2006).
[18] A. Tersigni, J. Shi, D. T. Jiang, and X. R. Qin, Phys. Rev. B **74**, 205326 (2006).
[19] J. Northrup, M. Tiago, and S. Louie, Phys. Rev. B **66**, 121404(R)(2002).
[20] D. Holmes, S. Kumaraswamy, A. Matzger, and K. P. C. Vollhardt, Chem. Eur. J. **5**, 3399, (1999).
[21] The point-spread function depends on setup conditions such as finite slit widths and beam illumination area. We use GIXD data for a single-crystal Si substrate bulk diffraction to estimate the function experimentally. The function is verified approximately as a Gaussian. The in-plane slit width setting is primarily responsible for the measured Gaussian width, and other setup conditions play minor roles in determining the Gaussian width.
[22] A. L. Patterson, Phys. Rev. **56**, 978 (1939).
[23] J. T. Sadowski, G. Sazaki, S. Nishikata, A. Al-Mahboob, Y. Fujikawa, K. Nakajima, R. M. Tromp, and T. Sakurai, Phys. Rev. Lett. **98**, 046104 (2007).
[24] T. A. Witten Jr. and L. M. Sander, Phys. Rev. Lett. **47**, 1400 (1981).
[25] A. Al-Mahboob, J. T. Sadowski, Y. Fujikawa, K. Nakajima, and T. Sakurai, Phys. Rev. B **77**, 035426 (2008).